

LEPTOGLUONS IN DILEPTON PRODUCTION AT THE LHC*

TOMASZ JELIŃSKI, DMITRY ZHURIDOV†

Institute of Physics, University of Silesia
Uniwersytecka 4, 40-007, Katowice, Poland

(Received October 21, 2015)

In the composite models with colored substructure of the fermions, the color singlet leptons are accompanied by a composite color octet partners, which are known as leptogluons. We consider the effect of leptogluons in the dilepton production at the LHC and show that in the reachable parameter range this effect is typically dominated by t -channel leptogluon exchange (indirect channel). We show that this channel alone can give a sizable contribution to the dimuon production at the LHC for TeV scale values of the invariant mass of $\mu^+\mu^-$ pairs.

DOI:10.5506/APhysPolB.46.2185

PACS numbers: 12.60.Rc, 13.85.Lg, 14.60.Hi

1. Introduction

For about a century, the particle physics has investigated matter at distances from about 10^{-10} m (size of the atom) to about 10^{-15} m (nucleons substructure), so it is five orders of magnitude progress in exploring the micro-world. A big question is what can happen next? Are presently known elementary particles complex at smaller distances? There are many interesting theories which explore physics at these tiny distances below 10^{-15} m, let us mention only theories of extra dimensions or string theories. Yet another type of models constitute the so-called composite models [1–8].

Early models, which introduced a substructure of the Standard Model (SM) leptons, were discussed in Refs. [4–8]. Leptons with colored subcomponents are automatically accompanied by color octet composites ℓ_8 having the same lepton numbers, which are called *leptogluons*. They can be probed at the high-energy collider experiments [9–11], in particular, at the LHC

* Presented by D. Zhuridov at the XXXIX International Conference of Theoretical Physics “Matter to the Deepest”, Ustroń, Poland, September 13–18, 2015.

† Corresponding author: dmitry.zhuridov@gmail.com

frontier [12–14]. Collider effects of the leptogluons are of exceptional interest since they are dominated by the tree level processes, while the related contact interactions and contributions to the lepton magnetic moments have one- and two-loop suppression, respectively.

The strongest mass bound for the charged leptogluons is $m_8 > 1.2\text{--}1.3$ TeV [14]. However, for the choice of parameters in Ref. [14], the t -channel production of leptogluons is suppressed with respect to their pair production. In this work, we show that for the compositeness scale Λ , which is close to the allowed values of m_8 , the t -channel exchange of leptogluons dominates over their pair production at 8 TeV LHC, and this channel alone can give a sizable contribution to the production of dileptons with the invariant mass $m(\ell^+\ell^-) = \mathcal{O}(1)$ TeV. (Here and below, m_8 denotes the relevant ℓ_8^\pm mass.)

2. Indirect and pair production of leptogluons at the LHC

The effective interaction of ℓ_8 with leptons and gluons can be written as¹ [15]

$$\mathcal{L} = \frac{g_s}{2\Lambda} \overline{\ell_8^A} \sigma^{\mu\nu} G_{\mu\nu}^A (a_{\ell L} P_L + a_{\ell R} P_R) \ell + \text{H.c.}, \quad (1)$$

where g_s is the strong coupling constant, $G_{\mu\nu}^A$ is the gluon field strength, $P_{L(R)}$ is the left (right) projector, $\ell = e, \mu, \tau$, $\sigma^{\mu\nu} = \frac{i}{2}[\gamma^\mu, \gamma^\nu]$, and for the new couplings, we take: $a_{\ell L} = 1$ and $a_{\ell R} = 0$ [14]. The width of the dominant decay of ℓ_8 can be written as $\Gamma_{\ell_8 \rightarrow g\ell} = \alpha_s m_8^3 / (4\Lambda^2)$.

The leading Feynman diagrams on the parton level for *indirect production* (IP) and *pair production* (PP)² of ℓ_8 in p - p collisions are shown in Figs. 1 and 2, respectively, and the total cross sections are (see Appendix A)

$$\hat{\sigma}_{gg \rightarrow \ell^+\ell^-} = \frac{\pi}{12} \alpha_s^2 \xi^4 m_8^2 F(r), \quad (2)$$

$$\hat{\sigma}_{q\bar{q} \rightarrow \ell_8^+ \ell_8^-} = \frac{16\pi}{9} \frac{\alpha_s^2}{m_8^2} r(1+2r)\beta, \quad (3)$$

$$\hat{\sigma}_{gg \rightarrow \ell_8^+ \ell_8^-} = \frac{\pi}{12} \frac{\alpha_s^2}{m_8^2} [F_1(r) + \xi^4 m_8^4 F_2(r) + \xi^2 m_8^2 F_{12}(r)], \quad (4)$$

where we have neglected terms of the order of $\mathcal{O}(\Gamma/m_8)$ with contributions below 1%, $\xi = a_{\ell L}/\Lambda$, $r = m_8^2/\hat{s}$ and $\beta = \sqrt{1-4r}$. Other functions are

¹ Notice that the effective compositeness scale for contact (4-fermion) interactions may exceed the scale Λ in Eq. (1) due to the loop factor, which was mentioned above. Notice that factor 1/2 in Eq. (1) leads to the Feynman rule without factor 2.

² Directly produced ℓ_8^\pm undergo $\ell_8^\pm \rightarrow \ell^\pm g$ decays with close to 100% branching ratios.

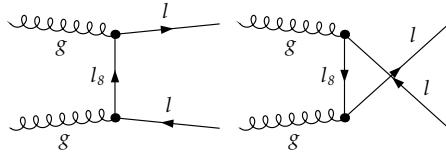


Fig. 1. Leading Feynman diagrams for $gg \rightarrow \ell^+ \ell^-$ via t -channel exchange of ℓ_8^\pm .

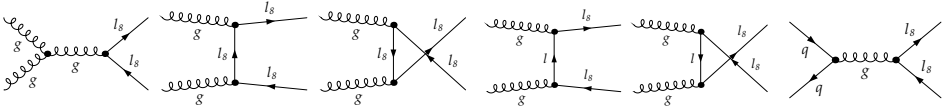


Fig. 2. Leading Feynman diagrams for the processes $gg \rightarrow \ell_8^+ \ell_8^-$ and $q\bar{q} \rightarrow \ell_8^+ \ell_8^-$.

defined as

$$F(r) = \frac{1 - 6r - 24r^2}{2r} + 3r(3 + 4r) \ln\left(\frac{1+r}{r}\right), \tag{5}$$

$$F_1(r) = -18r(4 + 17r)\beta + 54r(1 + 4r - 4r^2) \ln\left(\frac{1+\beta}{1-\beta}\right), \tag{6}$$

$$F_2(r) = \frac{4(1 - 4r)}{r} \left[(1 + 6r)\beta + 6r^2 \ln\left(\frac{1 - 2r + \beta}{1 - 2r - \beta}\right) \right], \tag{7}$$

$$F_{12}(r) = -3(2 + r)(1 + 6r)\beta + \frac{18r(1 + r)}{1 - r} \left[\ln\left(\frac{1 + \beta}{1 - \beta}\right) + r^2 \ln\left(\frac{1 - 2r + \beta}{1 - 2r - \beta}\right) \right]. \tag{8}$$

The total cross section for $pp \rightarrow abX \rightarrow cdX$ can be calculated as

$$\sigma_{pp \rightarrow cdX} = \int_{y_0}^1 \frac{dy}{y} \int_y^1 \frac{dx}{x} p_a(x, \mu_F^2) p_b\left(\frac{y}{x}, \mu_F^2\right) \hat{\sigma}_{ab \rightarrow cd}(ys), \tag{9}$$

where $y_0 = \mu_{cd}^2/s$ (μ_{cd} is the minimal invariant mass of cd), \sqrt{s} is the total energy of the proton–proton collisions, μ_F is the factorization scale, $p_a(x, Q^2) = x \text{pdf}_a(x, Q)$ is the parton a distribution in proton for the momentum transfer Q , and X represents the two jets close to the beam axis.

We have performed numerical calculations in MadGraph5 [22], using FeynRules [23, 24] to generate UFO-format [25] model files. Figure 3 shows cross sections for IP and PP³ of leptogluons at the LHC. In particular, IP of ℓ_8 dominates at 8 TeV LHC for $m_8 > 1.2$ TeV (current bound) and $\Lambda \sim m_8$.

³ The dependence of PP of ℓ_8 on Λ is due to the 4th and 5th diagrams in Fig. 2.

For $m_8 \approx 1$ TeV, the cross sections increase by factor of $\mathcal{O}(10)$ with the energy increase up to 14 TeV. For $m_8 \approx 2$ TeV, the PP (IP) cross section increases by factor of about 300 (~ 30) with the same energy increase.

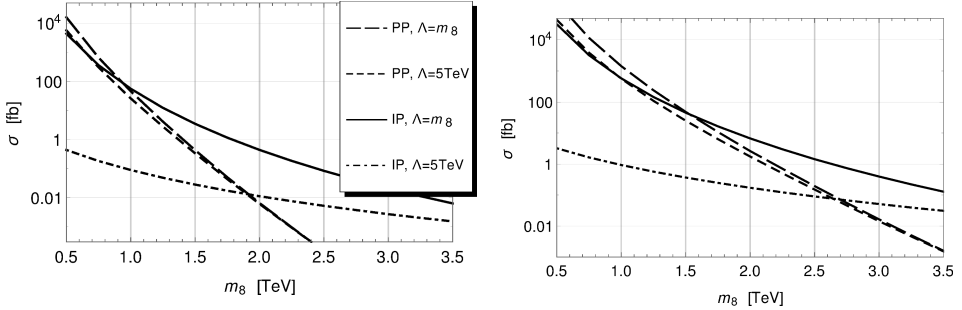


Fig. 3. Total cross sections for various processes that involve leptogluons *versus* the leptogluon mass m_8 for $\sqrt{s} = 8$ TeV (left) and 14 TeV (right). Solid (dot-dashed) and long-dashed (short-dashed) lines represent $pp \xrightarrow{\ell_8} \ell^+\ell^-$ and $pp \rightarrow \ell_8^+\ell_8^-$ processes for the compositeness scale $\Lambda = m_8$ ($\Lambda = 5$ TeV), respectively.

Figure 4 (left) shows the simulated dimuon invariant mass spectra at the LHC with $\sqrt{s} = 8$ TeV and 20.6 fb^{-1} of the integrated luminosity, where light, dark and white histograms represent Drell–Yan production (dominant SM background: Z/γ^*), the effect of muonic leptogluons μ_8^\pm with $m_8 = \Lambda = 1.5$ TeV and their combination, respectively. The difference between the number of events in the CMS data [26] and the number of simulated events normalized to the number of simulated events in various ranges of the invariant mass $m(\mu^+\mu^-)$ is shown in Fig. 4 (right). The solid line represents the SM background. The dashed line corresponds to the combination of

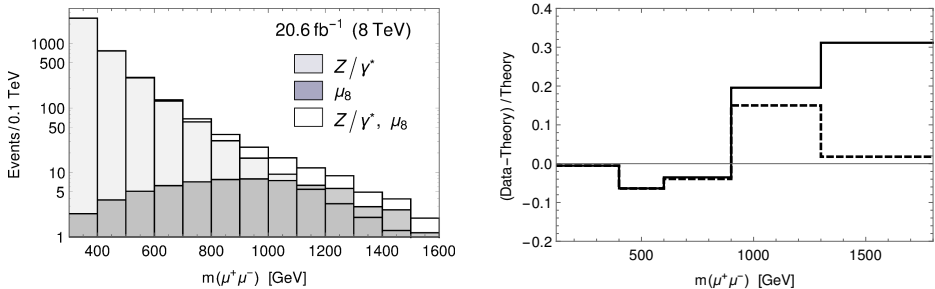


Fig. 4. Left: Simulated $\mu^+\mu^-$ invariant mass spectra. Right: Normalized difference between the number of the CMS data and simulated dimuon events in the given $m(\mu^+\mu^-)$ ranges for $\sqrt{s} = 8$ TeV and with 20.6 fb^{-1} . Solid (dashed) line is connected with the SM background (the SM background plus the signal of μ_8^\pm).

the SM background and the effect of IP of μ_8^\pm with the mass $m_8 = 2$ TeV and coupling-to-scale ratio $\xi = (2.4 \text{ TeV})^{-1}$, which minimizes the likelihood function: $\chi_{\min}^2 = 2.07$. Figure 4 shows that IP of μ_8 decreases the dimuon signal for large $m(\mu^+\mu^-)$.

To conclude, the present analysis shows a possibility of sizable effects of leptogluons in dilepton production at the LHC for large invariant masses.

We would like to thank Janusz Gluza and Henryk Czyż for collaborative work. This work was supported in part by the Polish National Science Centre, grant number DEC-2012/07/B/ST2/03867.

Appendix A

Indirect production of ℓ_8^\pm

Analytical results were derived with the help of FeynArts [16] and FormCalc [17]. Differential cross section for IP of leptogluons can be written as

$$\frac{d\hat{\sigma}_{gg\rightarrow\ell^+\ell^-}}{d\hat{t}} = \frac{1}{16\pi\hat{s}^2} \frac{1}{256} d_R g_s^4 \xi^4 \sum (\mathcal{M}_{11} + \mathcal{M}_{22}), \tag{A.1}$$

where the two summands (one of them is missing in Ref. [18]) correspond to the two diagrams in Fig. 1, $d_R = 8$ is the dimension of octet representation of SU(3), factor $1/256 = 1/(2^2 8^2)$ comes from the averaging over polarizations and colors of gluons, and normalized squared matrix elements are

$$\sum \mathcal{M}_{11} = -\frac{4\hat{t}^3(\hat{s} + \hat{t})}{(\hat{t} - m_8^2)^2}, \quad \sum \mathcal{M}_{22} = -\frac{4\hat{t}(\hat{s} + \hat{t})^3}{(\hat{u} - m_8^2)^2}, \tag{A.2}$$

where $\hat{s} = (k_1 + k_2)^2$, $\hat{t} = (q_1 - k_1)^2$ and $\hat{u} = (q_2 - k_1)^2$ are the Mandelstam variables, and \sum denotes the summation over initial and final spin states. Equation (2) can be derived using the formula

$$\hat{\sigma}_{gg\rightarrow\ell^+\ell^-} = \int_{-\hat{s}}^0 d\hat{t} \frac{d\hat{\sigma}_{gg\rightarrow\ell^+\ell^-}}{d\hat{t}}. \tag{A.3}$$

$\ell_8^+ \ell_8^-$ pair production

Following the method of Refs. [19–21] for $gg \rightarrow \ell_8^+ \ell_8^-$, we have

$$\begin{aligned} \frac{d\hat{\sigma}_{gg \rightarrow \ell_8^+ \ell_8^-}}{d\hat{t}} &= \frac{\pi\alpha_s^2}{16\hat{s}^2} \left[K_1(R) \sum (\mathcal{M}_{ss} + \mathcal{M}_{st} + \mathcal{M}_{su}) \right. \\ &\quad + K_2(R) \sum (\mathcal{M}_{tt} + \mathcal{M}_{uu}) + K_3(R) \sum \mathcal{M}_{tu} \\ &\quad + \xi^4 K_4(R) \sum (\mathcal{M}_{tt}^{\ell\ell} + \mathcal{M}_{uu}^{\ell\ell}) \\ &\quad \left. + \xi^2 K_5(R) \sum (\mathcal{M}_{st}^\ell + \mathcal{M}_{su}^\ell) + \xi^2 K_6(R) \sum \mathcal{M}_{tu}^\ell \right], \end{aligned} \tag{A.4}$$

where the terms with \mathcal{M}_{tt}^ℓ and \mathcal{M}_{uu}^ℓ are absent due to zero color factors, and the normalized squared matrix elements are given as follows

$$\sum \mathcal{M}_{ss} = \frac{(\hat{t} - m^2)(\hat{u} - m^2)}{\hat{s}^2}, \tag{A.5}$$

$$\sum \mathcal{M}_{st} = \frac{(\hat{t} - m^2)(\hat{u} - m^2) + m^2(\hat{u} - \hat{t})}{2\hat{s}(\hat{t} - m^2)} = \sum \mathcal{M}_{su}(\hat{t} \leftrightarrow \hat{u}), \tag{A.6}$$

$$\sum \mathcal{M}_{tt} = \frac{(\hat{t} - m^2)(\hat{u} - m^2) - 2m^2(\hat{t} + m^2)}{2(\hat{t} - m^2)^2} = \sum \mathcal{M}_{uu}(\hat{t} \leftrightarrow \hat{u}), \tag{A.7}$$

$$\sum \mathcal{M}_{tu} = -\frac{m^2(\hat{s} - 4m^2)}{2(\hat{t} - m^2)(\hat{u} - m^2)}, \tag{A.8}$$

$$\sum \mathcal{M}_{tt}^{\ell\ell} = \frac{(\hat{t}\hat{u} - m^4)(\hat{t} - m^2)^2}{4\hat{t}^2} = \sum \mathcal{M}_{uu}^{\ell\ell}(\hat{t} \leftrightarrow \hat{u}), \tag{A.9}$$

$$\begin{aligned} \sum \mathcal{M}_{st}^\ell &= \frac{\hat{t}\hat{u} - 4\hat{t}^2 + \hat{u}^2 + m^2(13\hat{t} - \hat{u})}{8\hat{s}} - m^4 \frac{8\hat{t} + \hat{u} - 4m^2}{4\hat{s}\hat{t}} \\ &\quad - 5m^2 \frac{\hat{t} - m^2}{8\hat{t}} = \sum \mathcal{M}_{su}^\ell(\hat{t} \leftrightarrow \hat{u}), \end{aligned} \tag{A.10}$$

$$\begin{aligned} \sum \mathcal{M}_{tu}^\ell &= \left[-\frac{(\hat{t}\hat{u} - m^4)(\hat{t} + 2m^2)}{8(\hat{t} - m^2)\hat{u}} \right. \\ &\quad \left. + m^2 \frac{\hat{t}\hat{u} - 4\hat{u}^2 + 2m^2(3\hat{t} + 7\hat{u}) - 17m^4}{8(\hat{t} - m^2)\hat{u}} \right] + [\hat{t} \leftrightarrow \hat{u}], \end{aligned} \tag{A.11}$$

where $m \equiv m_8$, and the nonvanishing color factors can be written as

$$K_1(R) = d_R C_A C_F = 72, \quad K_2(R) = d_R C_F^2 = 72, \tag{A.12}$$

$$K_3(R) = d_R C_F [C_A - 2C_F] = -72, \tag{A.13}$$

$$K_4(R) = 64, \quad K_5(R) = -K_6(R) = 24, \tag{A.14}$$

where C_A and C_F are the Casimir invariants. In our case of SU(3) octets, we have $d_R = 8$ and $C_A = C_F = 3$. Equation (4) can be derived using the formula

$$\hat{\sigma}_{gg \rightarrow \ell_8^+ \ell_8^-} = \int_{m^2 - \frac{\hat{s}}{2}(1+\beta)}^{m^2 - \frac{\hat{s}}{2}(1-\beta)} d\hat{t} \frac{d\hat{\sigma}_{gg \rightarrow \ell_8^+ \ell_8^-}}{d\hat{t}}. \quad (\text{A.15})$$

The terms that include ξ in Eq. (A.4) are new analytical results related to the 4th and 5th diagrams in Fig. 2 and their interference with other diagrams.

The differential cross section for $q\bar{q} \rightarrow \ell_8^+ \ell_8^-$ is given in Ref. [12]. However, there is a misprint in Ref. [12] concerning the interference terms in Eq. (A.6).

REFERENCES

- [1] J.C. Pati, A. Salam, *Phys. Rev. D* **10**, 275 (1974) [*Erratum ibid.* **11**, 703 (1975)].
- [2] H. Terazawa, K. Akama, Y. Chikashige, *Phys. Rev. D* **15**, 480 (1977).
- [3] M.A. Shupe, *Phys. Lett. B* **86**, 87 (1979).
- [4] H. Harari, *Phys. Lett. B* **86**, 83 (1979).
- [5] E.J. Squires, *Phys. Lett. B* **94**, 54 (1980).
- [6] H. Harari, N. Seiberg, *Phys. Lett. B* **98**, 269 (1981).
- [7] R. Barbieri, L. Maiani, R. Petronzio, *Phys. Lett. B* **96**, 63 (1980).
- [8] H. Fritzsch, G. Mandelbaum, *Phys. Lett. B* **102**, 319 (1981).
- [9] M.A. Abolins *et al.*, *eConf* **C8206282**, 274 (1982).
- [10] J.L. Hewett, T.G. Rizzo, *Phys. Rev. D* **56**, 5709 (1997) [arXiv:hep-ph/9703337].
- [11] J.L. Abelleira Fernandez *et al.* [LHeC Study Group], *J. Phys. G* **39**, 075001 (2012) [arXiv:1206.2913 [physics.acc-ph]].
- [12] A. Celikel, M. Kantar, S. Sultansoy, *Phys. Lett. B* **443**, 359 (1998).
- [13] T. Mandal, S. Mitra, *Phys. Rev. D* **87**, 095008 (2013) [arXiv:1211.6394 [hep-ph]].
- [14] D. Goncalves-Netto *et al.*, *Phys. Rev. D* **87**, 094023 (2013) [arXiv:1303.0845 [hep-ph]].
- [15] K.A. Olive *et al.* [Particle Data Group], *Chin. Phys. C* **38**, 090001 (2014).
- [16] T. Hahn, *Comput. Phys. Commun.* **140**, 418 (2001) [arXiv:hep-ph/0012260].
- [17] T. Hahn, M. Perez-Victoria, *Comput. Phys. Commun.* **118**, 153 (1999) [arXiv:hep-ph/9807565].

- [18] A.N. Akay, H. Karadeniz, M. Sahin, S. Sultansoy, *Europhys. Lett.* **95**, 31001 (2011) [arXiv:1012.0189 [hep-ph]].
- [19] B.L. Combridge, *Nucl. Phys. B* **151**, 429 (1979).
- [20] H.M. Georgi, S.L. Glashow, M.E. Machacek, D.V. Nanopoulos, *Ann. Phys.* **114**, 273 (1978).
- [21] H. Tanaka, I. Watanabe, *Int. J. Mod. Phys. A* **7**, 2679 (1992).
- [22] J. Alwall *et al.*, *J. High Energy Phys.* **1106**, 128 (2011) [arXiv:1106.0522 [hep-ph]].
- [23] N.D. Christensen, C. Duhr, *Comput. Phys. Commun.* **180**, 1614 (2009) [arXiv:0806.4194 [hep-ph]].
- [24] A. Alloul *et al.*, *Comput. Phys. Commun.* **185**, 2250 (2014) [arXiv:1310.1921 [hep-ph]].
- [25] C. Degrande *et al.*, *Comput. Phys. Commun.* **183**, 1201 (2012) [arXiv:1108.2040 [hep-ph]].
- [26] V. Khachatryan *et al.* [CMS Collaboration], *J. High Energy Phys.* **1504**, 025 (2015) [arXiv:1412.6302 [hep-ex]].